Silicide formation at the Ti/Si(111) interface: Room-temperature reaction and Schottky-barrier formation

M. del Giudice, J. J. Joyce, M. W. Ruckman, and J. H. Weaver
Department of Chemical Engineering and Materials Science, University of Minnesota, Minneapolis, Minnesota 55455
(Received 23 July 1986)

High-resolution core-level synchrotron-radiation photoemission has been used to study the evolving Ti/Si(111)-2×1 interface at room temperature. Si 2*p* core-level results show extended intermixing and reaction following the Ti-induced disruption of the Si surface. Three reacted components are identified, shifted to lower binding energy relative to the substrate by 350, 625, and 1125 meV. These core-level results have been decomposed to obtain the intensity of each component as a function of coverage and determine the component-specific attenuation curves. Modeling of the attenuation curves shows that the first shifted species is associated with a bonding configuration of empirical formula $TiSi_4$ and forms only during the deposition of the first angstrom of Ti. The second component is associated with TiSi, and this phase forms in the coverage range $0.5 \leq \Theta \leq 8$ Å. The final Si configuration reflects a phase of variable stoichiometry and binding energy, corresponding to a solution of Si in Ti. Titanium metal accumulates at coverages above ~14 Å. The profile and morphology of this heterogeneous interface is controlled by Ti and Si diffusion through the reaction products and their grain boundaries. These chemical changes in the interface have been correlated with measurements of the variation in the Schottky-barrier height.

INTRODUCTION

Although metal-semiconductor interfaces are ubiquitious in microelectronic thin-film technologies, our understanding of the detailed physics and chemistry of interface formation is far from complete.[1] The importance of interface properties has stimulated numerous basic studies of such fundamental issues as adatom clustering,[2,3] chemical bonding and reaction thresholds,[4,5] atomic intermixing,[6] heterogeneous growth morphologies,[7,8] and Schottky-barrier formation.[9,10] Indeed, a variety of different techniques have been used to define the microscopic details.[11] Many of these have sought to characterize the macroscopic parameters controlling interface growth so that greater control could be gained over the microscopic profiles of these interfaces. The main problem encountered is that most of the properties of the junction are determined by ultrathin layers which may be only a few angstroms wide.

In this paper we discuss high-resolution synchrotron-radiation photoemission results for the evolving Ti/Si(111) interface. With these experimental results, we formulate a model for the morphology of the interface. These studies build on what has been reported for other systems where multiphase interfaces are formed, including photoemission results for V/Ge(111),[12–14] Ce/Ge(111),[15–16] Ce/Si(111),[17] and Co/Si(111).[18] An important aspect of the present results is that the Si 2*p* core-level resolution is significantly better than in any previous study, allowing improved line-shape decomposition and analysis. This has made it possible to investigate the assertion that local reactions at interfaces can result in the formation of well-defined chemical species. We find that this assertion is fundamentally sound. We also find evidence for solid solution phase formation. In this paper, we restrict ourselves to the room-temperature behavior of Ti/Si; studies of the kinetics of interface formation and diffusion are discussed elsewhere.[19]

Previous studies of Ti/Si(111)-2×1 which used medium-energy ion scattering (MEIS) (Ref. 20) and electron-energy-loss spectroscopy (EELS) (Ref. 21) showed that Ti reacts with silicon at room temperature to form an interface reaction product which has an average composition of TiSi. The MEIS results also indicated that an interlayer of displaced Si atoms ~2 Å thick is present between TiSi and the substrate. Although the MEIS results indicated immediate reaction at the interface, the EELS results showed that intermixing between Ti and Si was triggered at a nominal coverage of ~2 Å. The results by Butz *et al.*[22] showed that the evolution of the interface was highly dependent on the presence of oxygen. Studies conducted at higher temperature demonstrated that TiSi, which initially forms at the interface, will ultimately convert to $TiSi_2$, the most stable silicide.[23,24]

In our studies, we were particularly interested in the behavior of the interface at low coverage, including the triggering of reaction and the heterogeneous-homogeneous nature of the reaction product. This is important for understanding interface development because the morphology at the earliest stages of reaction determines the microstructure of the reaction product and, subsequently, diffusion, kinetics, and thermal stability.[19,20,22] Our results show that reaction has been initiated for coverages as low as 0.25 Å and that interface evolution is highly heterogeneous until ~8 Å. Reaction ceases or is sharply curtailed because room-temperature diffusion is unable to provide Si atoms in sufficient number for silicide formation. Accumulating metal atoms then bury the intermixed or silicide region, with an error-function-like con-

centration profile of Si in solution in this growing Ti layer. We found no evidence for segregation of Si on the Ti surface. With the information gained from modeling of the interface, we can correlate the formation of the Schottky barrier with morphology and interface chemistry.

EXPERIMENTAL TECHNIQUES

Photoemission experiments were conducted at the Tantalus light source at the Wisconsin Synchrotron Radiation Center using the "grasshopper" Mark II monochromator and beamline. Photoelectron energy analysis was done with a double-pass cylindrical mirror analyzer.[25] Changes in the chemical character of Si atoms at the Ti/Si(111) interface were identified by chemical shifts in the Si $2p$ core emission. These core-level spectra were recorded at photon energies of 108, 112, 120, and 135 eV to vary the surface sensitivity of the measurements. High-resolution studies were done for $0 \leq \Theta \leq 30$ Å with an overall resolution (monochromator plus analyzer) of 188 meV at $h\nu = 108$ eV, 287 meV at 112 eV, and 317 meV at 120 eV. Studies at 135 eV were done with an overall resolution of 430 meV because of the low-photon flux. Particularly detailed studies were conducted for $0 \leq \Theta \leq 3$ Å.

Si parallelepipeds (n-type, 5—10 Ω cm) were notched, and cleaved *in situ* to obtain clean Si(111)-2×1 surfaces. The Ti source was a slice ($\sim 1 \times 1 \times 8$ mm^3) of high-purity, beam-melted ingot metal which was sublimed from a 5-mil Ta boat (100—120 Å). During evaporation, the pressure in the system rose from an operating pressure of $\sim 5 \times 10^{-11}$ to 2×10^{-10} Torr or less (sample to source distance ~ 30 cm, rate of deposition ~ 1 Å/min). In this paper, we use angstrom units to refer to nominal coverages where 1 Å = 0.8 ML = 5.76×10^{14} atoms/cm^2 as referenced to the surface density of Si(111). At the same time, it should be clear that the thickness of the reacted interface is only approximated by these nominal coverages.

EXPERIMENTAL RESULTS

In Fig. 1 we report results for bulk-sensitive Si $2p$ core-level emission as a function of Ti coverages as measured at $h\nu = 108$, 112, and 120 eV. These core-level energy distribution curves (EDC's) are corrected for band bending, as will be discussed later in this paper (an initial band bending of 250 meV was achieved by 2 Å, but the shift is reversed after $\Theta = 2$ Å). At a photon energy of 108 eV (right panel), the electron kinetic energy in the sample is ~ 9 eV, corresponding to a photoelectron mean-free path of $\lambda \sim 25$ Å. At 112 eV, the mean-free path is ~ 12 Å and it decreases to ~ 6 Å at 120 eV. Thus, the EDC's of Fig. 1 probe different thicknesses of the interface and provide complementary information about the reacting region.

The results for 108 eV show that Si at the interface undergoes a chemical reaction for $\Theta < 1$ Å. Although it is difficult to determine the number of chemical species present with this photon energy (because of the long mean-free path), we see a shoulder at ~ 0.6 eV lower

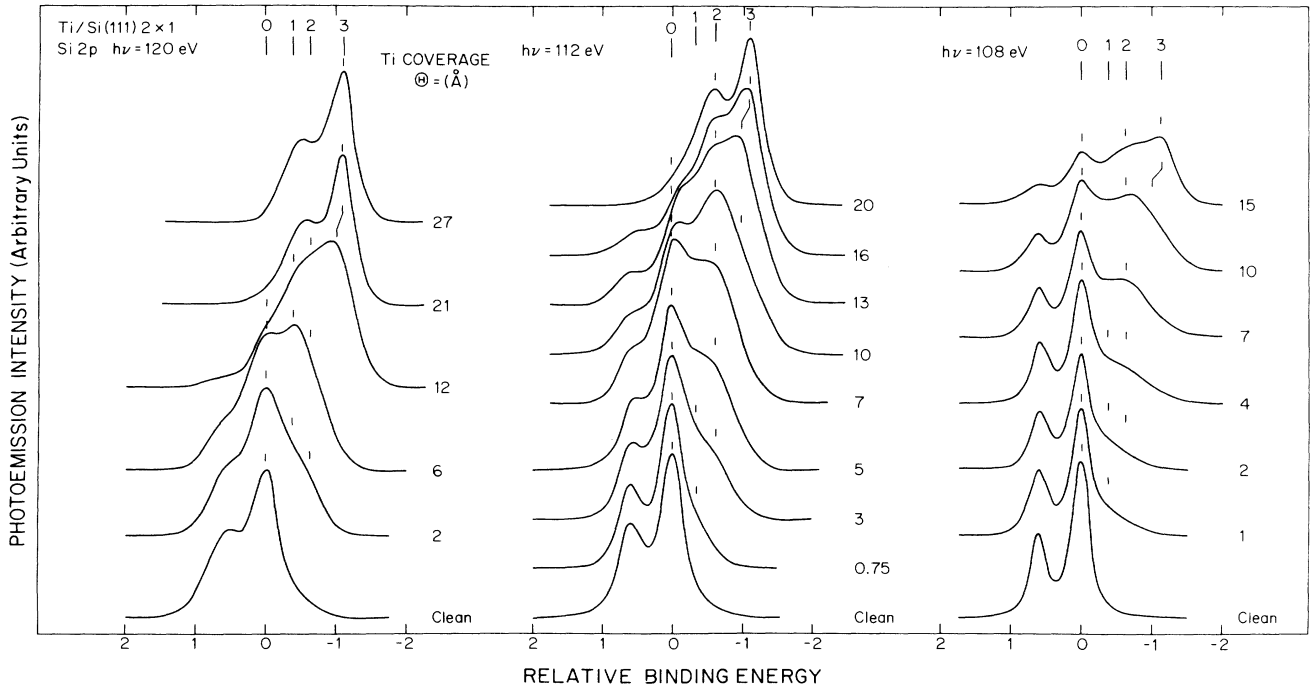

FIG. 1. Si $2p$ core-level EDC's for the Ti/Si(111)-2×1 interface as a function of Ti coverage for $h\nu = 108$, 112, and 120 eV. Photoemission spectra have been background subtracted, normalized, and corrected for band-bending effects. As shown, three reacted components (labeled 1, 2, 3) and the substrate (0) are formed at the interface. The binding energy of component 3 decreases with coverage, indicating a solid solution of Si in Ti. The energies of components 1 and 2 are fixed.

binding energy than for the bulk Si $2p$ core level for $1 \leq \Theta \leq 7$ Å. After 7 Å, another component grows, as indicated by tic mark 3. This feature dominates the experimental spectra by 15-Å coverage and appears at a fully shifted position of 1.125 eV lower binding energy relative to bulk Si.

The results taken with greater surface sensitivity at 112 eV show that the shoulder at 0.6 eV is actually the sum of two components, indicated by tic marks 1 and 2. (The substrate emission is labeled "0".) For coverages below 1 Å, there is broadening of the Si $2p$ core emission due to the first chemically shifted component at -0.35 eV. For $\Theta > 1$ Å, there is a second reacted component which appears at -0.63 eV. This grows until ~ 10-Å nominal coverage and then gradually yields to the final component at -1.12 eV. As shown, the experimental line shape is that of a single, well-defined, spin-orbit-split doublet by about $\Theta = 20$ Å. This convergence to a single species is even more evident in the left panel of Fig. 1 where results with higher surface sensitivity show the spin-orbit splitting to be 0.6 eV and the branching ratio to be ~ 0.5, as measured with $h\nu = 120$ eV. Analogous spectra taken with lower resolution at $h\nu = 135$ ($\lambda \sim 4.5$ Å) support these observations (not shown). The results summarized in Fig. 1 demonstrate that complicated chemical processes occur at ultralow coverage when Ti atoms are deposited onto cleaved Si(111) surfaces. Three distinct reacted species are observed, consistent with what has been found for other reactive interfaces.

To determine the coverage-dependent behavior of each of the interface species at the Ti/Si interface, we have performed core-level decompositions of the results reported in Fig. 1. To do so, however, it was first necessary to determine the line shape for the clean surface as a function of photon energy, with account taken of surface-shifted atoms. This was done by decomposing the spectra into spin-orbit components to determine the total Si $2p_{3/2}$ emission, as shown in Fig. 2 for different photon energies. The bottom EDC shows the sum of the $2p_{1/2}$ and $2p_{3/2}$ emission while the others show only the $2p_{3/2}$ contribution (dashed line). Further analysis required determination of the intrinsic linewidth of the $2p_{3/2}$ level. For that, we used the full width at half maximum (FWHM) measured at 108 eV where the contribution from surface atoms was minimal (less than 5% of the total signal). We then deconvolved the spectra using a Gaussian transmission function for the experimental apparatus response function and found the Si $2p_{3/2}$ intrinsic width to be ~ 200 meV. We could then account for experimental broadening for other photon energies and decompose the experimental Si $2p_{3/2}$ emission at 112, 120, and 135 eV. The results are summarized in Fig. 2 where the solid lines are the line shape of the intrinsic emission broadened by the apparatus and the shaded regions are the difference between the measured spectra (dashed) and the broadened, intrinsic emission. As has been discussed by others,[26–28] the difference corresponds to emission from surface atoms, the contribution of which increases with surface sensitivity. Two surface core-level shifts can be identified in Fig. 2 with relative energy shifts of -0.3 eV (labeled S_2) and 0.25 eV (S_1). These two components are associated with the rearrangement of atoms bonding in the first layer of Si due to the (2×1) reconstruction of the surface.

To check our procedure for determining the surface components and their relative intensities, we used the ratio of surface to bulk Si $2p_{3/2}$ emission to find the photoelectron escape depth at the different photon energies. Using an average distance between layers for Si along the [111] direction of $d_\perp = 1.57$ Å, it can be shown that the surface to bulk intensity ratio is given by

$$R = I_S / I_B = \exp(d_\perp / \lambda) - 1 .$$

The results for the mean-free paths and the intensity ratios for different photon energies are reported in Table I. These results indicate good agreement between our experimentally estimated λ values and those summarized by Seah and Dench.[29]

Once the experimental line shape for the substrate is

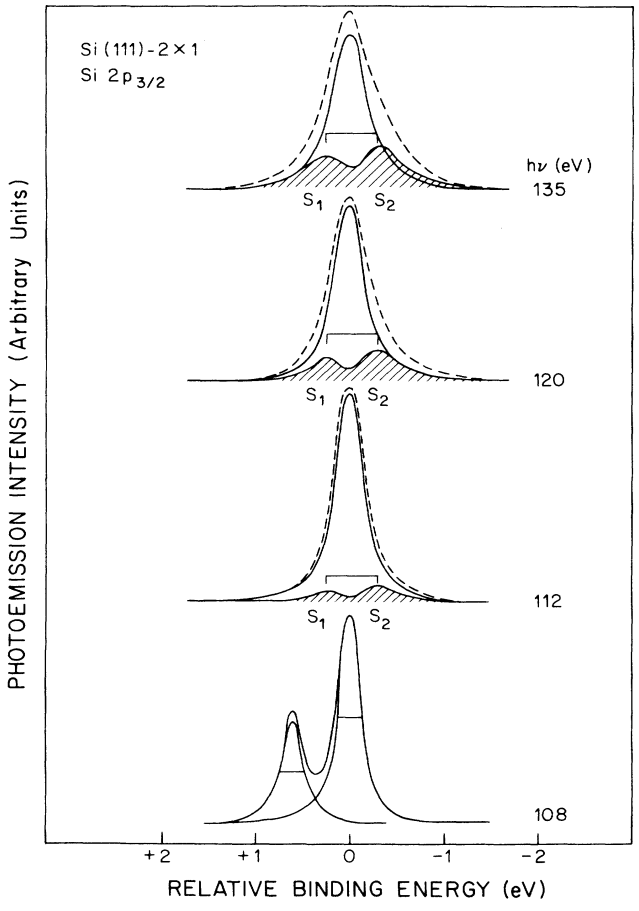

FIG. 2. Line-shape analysis results for the clean Si(111)-2×1. The bottom-most spectrum shows the total Si $2p$ emission as measured with a bulk-sensitive energy of $h\nu = 108$ eV. The spin-orbit splitting is 0.6 eV and the branching ratio is 0.5. Analysis of the Si $2p_{3/2}$ component with greater surface sensitivity (112, 120, 135 eV) shows at least two surface-shifted Si $2p_{3/2}$ core-level components (dashed areas). The surface-to-bulk intensity ratios were used to determine the photoelectron mean-free paths (Table I).

TABLE I. Comparison between experimental escape depths at different photon energies as calculated by the surface-to-bulk intensity ratio and the literature values summarized by Ref. 29.

$h\nu$ (eV)	108	112	120	135
Surface-to-bulk intensity ratio	$<5\%$	15.5%	28%	46%
λ_{expt} (Å)	>25	10.9	6.3	4.2
$\lambda_{(Ref.\ 29)}$ (Å)	24	11.8	6.0	4.36

determined under our measurement conditions, we can decompose the spectra presented in Fig. 1 for each coverage. In the left panel of Fig. 3 we show Si $2p$ results for $0 \leq \Theta \leq 3$ Å taken at $h\nu = 112$ eV. As can be seen from the raw data, core-level modification starts at the lowest coverage reported, 0.25 Å. On the right-hand side of Fig. 3, we show the results of decomposition of total emission to obtain the Si $2p_{3/2}$ contribution. That analysis indicates that the first reacted component is shifted -0.35 eV and is responsible for the broadening of the total Si $2p$ emission for $0 < \Theta \leq 0.75$. The contribution from this species grows steadily until $\Theta = 1$ Å when a second component appears at even lower binding energy (shaded area at -0.625 eV). Together these two components are responsible for the enhancement of the shoulder seen at $\Theta = 3$ Å.

In Fig. 4, we present the results of the decomposition procedure for the Si $2p_{3/2}$ emission at $h\nu = 108$ eV (left) and 112 eV (right) showing the evolution at higher coverage. The second reacted component (labeled 2) appears by ~ 1 Å of Ti coverage and grows until 7–8 Å. To obtain satisfactory fits with experiment, this second component was continuously broadened with Ti coverages up to 3–4 Å where its full width at half maximum saturates at a value of 0.85 eV for both photon energies presented. This

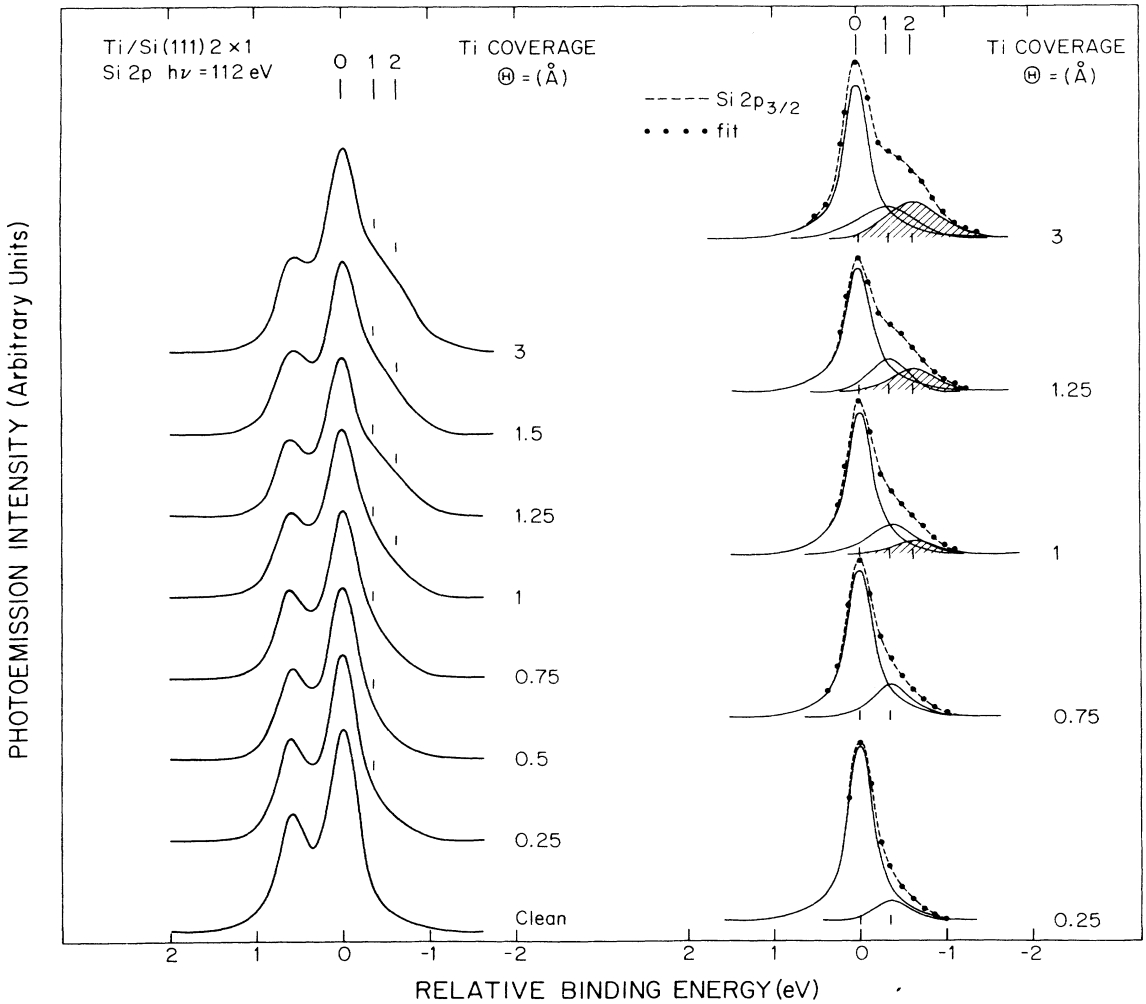

FIG. 3. Si $2p$ EDC's at $h\nu = 112$ eV for $0 \leq \Theta \leq 3$ Å of Ti (left panel) and representative decompositions (right panel). For the decompositions, the experimental curve is given by a dashed line, the different contributions are given by solid lines, and the total is given by the solid circles. As shown, the first reaction product is present at very low coverage ($\Theta = 0.25$ Å), indicating an immediate reaction with the substrate. For $\Theta < 1$ Å only one reacted component is present at -350 meV. After 1 Å of Ti, a second reacted component is present at -0.625 eV (shaded contribution).

indicates that there are a number of inequivalent sites present in the reacted film but that there is an overall average configuration indicated by the fixed kinetic energy of this reaction product. It is also noteworthy that the ratio of the substrate emission (labeled 0) to the first reacted product (labeled 1) is approximately constant for nominal Ti coverages of 1–5 Å and that the second reaction product grows relative to the others.

Interestingly, the behavior of the third reacted component is quite different from that of the second. In particular, its emission spectrum sharpens with metal coverages while growing in relative intensity, as is evident from

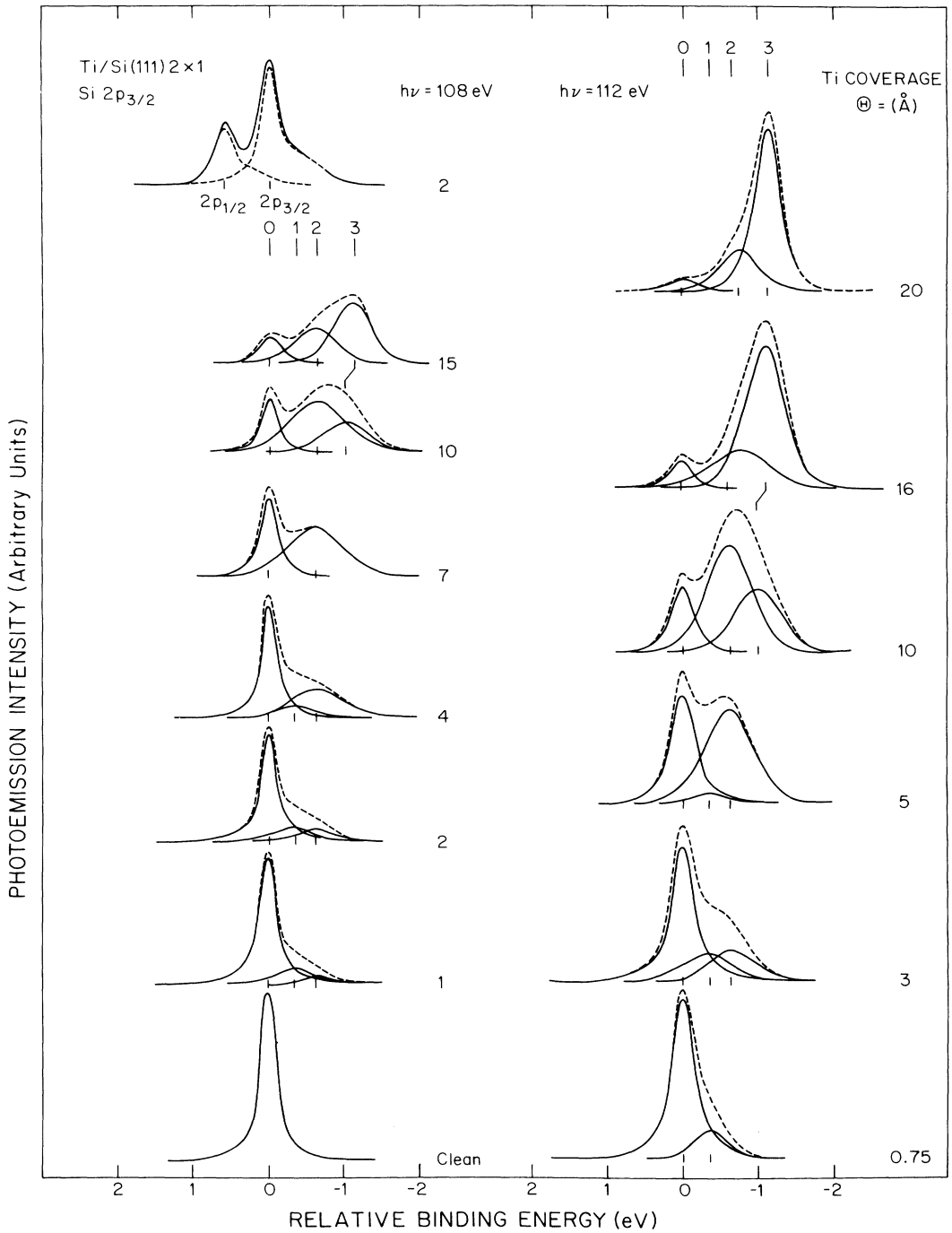

FIG. 4. Left panel: Decomposition results for some of the EDC's presented in Fig. 1 for $h\nu = 108$ eV. The topmost spectrum show the decomposition of the Si $2p$ into the spin-orbit-split pair. The other results are for the Si $2p_{3/2}$ component since the $2p_{1/2}$ component has been stripped away, as discussed in the text. Right panel: Representative Si $2p_{3/2}$ decompositions for $h\nu = 112$ eV. Comparison with analogous coverages in the left panel shows the effect of greater surface sensitivity.

Fig. 4. Indeed, the FWHM goes from ~ 0.75 eV at $\Theta = 10$ Å to 0.375 eV at 20 Å of coverage for 112 eV photon energy. Moreover, the energy position of this feature is not constant but shifts from ~ -1 eV to -1.125 eV with increasing Ti coverage in the range $10 \leq \Theta \leq 15$ Å. This indicates that the silicon atoms are in an environment which varies with coverage such that Si is ultimately completely isolated in the Ti matrix. Analogous behavior has been reported for Ga atoms at metal-GaAs interfaces, but the present results are the first to show the chemical shift associated with the dilution of Si in the final metal-silicon reaction product. We believe that this solution phase will be observed in other systems when sufficiently high-resolution studies are undertaken. Likewise, the broadening needed to adequately fit component 2 reflects inequivalent sites in the reaction product but could not be seen at lower resolution.

DISCUSSION

To be more quantitative in our characterization of the Ti/Si(111) interface results, we plot in Fig. 5 the attenuation curves $\ln[I(\Theta)/I(0)]$ for each Si species as measured with $h\nu = 108$ eV and 112 eV. $I(0)$ is the integrated Si $2p$ emission from the cleaved surface. The topmost curve in each panel refers to the total Si $2p$ attenuation. The behavior of each reacted species can be seen from the component-specific attenuation curves, labeled 0–3 in accord with the previous figures. In the following, we emphasize the results for 112 eV; equivalent information can be extracted from those at 108 eV with differences related to mean-free paths.

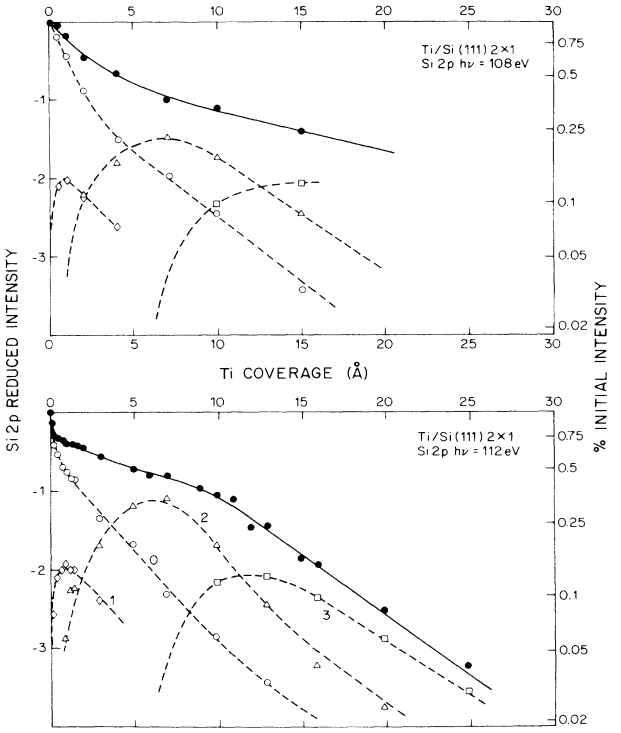

FIG. 5. Core-level attenuation curves showing $\ln[I(\Theta)/I(0)]$ as a function of coverage Θ for $h\nu = 108$ eV (top panel) and $h\nu = 112$ eV (bottom panel). The topmost curve in each panel (solid line with experimental points given by solid symbols) shows the behavior of the total Si $2p$ emission. The open symbols correspond to the component-specific attenuation curves such that the intensity of each component is given by the decomposition of the results of Fig. 1. The dashed lines are results of the modeling and show excellent agreement with experiment.

In the coverage range $0 \leq \Theta \leq 1$ Å, we see that there is a sharp drop in the integrated Si $2p$ intensity for 112 eV (less evident at 108 eV where $\lambda \sim 25$ Å). Between about 1 and 10 Å, the total signal is attenuated with a slope corresponding to a $1/e$ decay length of ~ 13 Å. Near 10 Å, there is a second inflection in the total attenuation curve and, thereafter, the intensity drops with a characteristic decay length of ~ 8 Å. These observations, which are typical for many reacted interfaces,[1,4,11–18] are not very informative unless the different contributions to the total intensity can be distinguished. The results of the line-shape decompositions show that the first reacted component grows in the region $0 \leq \Theta \leq 1.5$ Å and saturates at about 15% of the total signal. At the same time, the second reacted component grows after a nominal coverage of about 1 Å. This second component attenuates the emission from the first and the substrate itself, giving them apparent decay lengths of ~ 3.5 Å (lower panel). The growth of the third reacted species causes the attenuation of those beneath it. Ti metal starts to accumulate when the nominal Ti coverage exceeds about 14 Å, and the Si $2p$ signal from the reacted interface then decays with $\lambda \sim 8$ Å. These results make possible the following observations (see Ref. 16 for a discussion of generic attenuation curves and interface morphologies).

(1) There is a pattern of sequential reaction such that each phase grows, saturates, and is then attenuated by another which grows over it.

(2) The different phases do not consume each other. This can be seen from the consistency of the attenuation of the substrate and the reacted species in each characteristic coverage region. For example, if the growth of the third reacted species were at the expense of the underlying species, then the slope from species 2 for $7 \leq \Theta \leq 13$ Å would be smaller than that of the substrate, in contrast to what is observed.

(3) The rate at which the substrate is consumed diminishes with increasing coverage. This can be seen from the attenuation curves by noting the rapid decay of the substrate component at low coverage (relatively few adatoms can bond with many Si atoms and thereby convert them to the chemically shifted components) and the more gradual decay at high coverage (fewer substrate atoms are needed to form the metal-rich reaction product and reaction is limited by diffusion).

In previous studies,[13,16,17] we have shown that a quantitative understanding of interface evolution and properties can be obtained by modeling the interface as a series of reaction products. We have argued that there will be reaction-driven diffusion across the interface once reaction at an interface is initiated. The source of the semiconductor atoms is the disrupting substrate itself, which is

effectively infinite, but there are kinetic limitations on the growth of the overlayer. When the number of semiconductor atoms is sufficient to satisfy mass balance, a single phase described by the equation $xM+yS \rightarrow M_xS_y$ will form, where x and y denote the number of metal and semiconductor atoms, M and S, respectively. On the other hand, a second reaction product will form when semiconductor atom diffusion through the reacted overlayer is unable to balance the number of metal atoms arriving at the surface. Two reacted species can form simultaneously because the interface is morphologically heterogeneous. In modeling this reaction, it is necessary to partition the arriving metal atoms between the two phases. This has been approximated by a linear lever rule described by[16]

$$\chi=(\Theta-\Theta_2)/(\Theta_1^*-\Theta_2) ,$$

where Θ is the metal coverage, Θ_2 is the coverage at which the second phase starts to form, and Θ_1^* is the coverage at which the first phase stops. This process assumes that each reaction product has a distinct stoichiometry. If there are more than two phases which form sequentially, the process can be iterated until the semiconductor content of the overlayer becomes negligible and the overlayer converges to the pure metal. On the basis of these assumptions, a set of equations describing the relationship between the photoemission signal (attenuation curves) and the morphology and chemistry of the interfaces can be derived, as described in detail in Ref. 16.

The experimental results for the Ti/Si(111) indicate that this type of modeling would be appropriate for the first two reaction products and that it would yield the coverages and stoichiometries for those two products. The results also show, however, that the third or final Si bonding configuration changes with coverage and can be described as a solution of Si in Ti. The assumption of fixed stoichiometry therefore breaks down, and the lever rule approximation is not valid. For the purpose of fitting attenuation curves of the sort shown in Fig. 5, however, the concentration profile can be approximated by a phase with distinct concentration which grows simultaneously with TiSi at the beginning and with Ti at the end. We have adopted this procedure, noting that it gives greater uncertainty in the onset and completion coverages and no quantitative information about the solution stoichiometry.

In Fig. 6 we report schematically the results of the fitting procedure. As discussed above, the experimental results show that one phase forms and then yields to another; the stages at which the evolution occurs are given by the quantitative modeling. The x axis corresponds to the nominal coverage, Θ. The left vertical axis gives the Si content of the overlayer (solid line) and the right vertical axis gives the Ti content (dashed line). Error bars in determining stoichiometries are also shown. The solid solution is sketched for coverages exceeding about 6 Å as being richer in Si close to the TiSi layer and converging to pure Ti at about 14 Å. The circular insets give our picture of the developing morphology of the interface.

With reference to Fig. 6, the formation of the Ti/Si(111) interface can be described as follows.

(1) Coverage range 0—0.5 Å. When Ti atoms are first deposited onto the semiconductor surface, they react according to the chemical equations $M+3S \rightarrow MS_3$ or $M+4S \rightarrow MS_4$, where M denotes metal and S denotes semiconductor atoms. We have found the best agreement between the model and the experimental results when the Si concentration is between 75% and 80% for the first species; with this uncertainty, we refer to it hereafter as $TiSi_4$. This species forms on the surface at the lowest coverage, probably as patches as Ti atoms disrupt the Si substrate. With increasing coverage, this disruption spreads across the surface but appears to be complete by about 1 Å. The character of these patches is most difficult to demonstrate definitively, given their very limited thickness. We believe that this region represents the true transition region between the crystalline, pure Si substrate, and the silicides which grow at higher coverage.

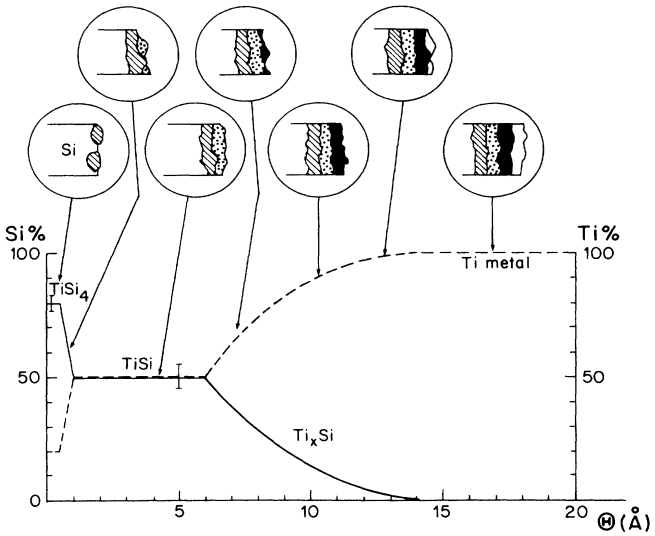

FIG. 6. Schematic of Ti/Si(111)-2×1 interface evolution. The left axis corresponds to the Si content in atomic percent and the right axis is the Ti content. The circled insets show the morphology at different stages of film growth. At lowest coverage we see the heterogeneous $TiSi_4$ phase, the changeover to the formation of TiSi, and the grading into the Si-in-Ti solution phase. The coverages at which these changes occur are given in Å by the x axis.

(2) Coverage range 0.5—1 Å. This region corresponds to the onset of silicide formation. In particular, there are now competing processes which occur, namely the completion of the $TiSi_4$ transition region and the development of the silicide. The two parallel reactions are described by $M+4S \rightarrow MS_4$ and $M+S \rightarrow MS$ where we find that the silicide corresponding to the second chemically shifted species is very close in composition to TiSi. The linear decrease in the Si concentration shown in Fig. 6 in the two-phase region from 0.5 to 1 Å results from the assumption that the partitioning of the metal atoms when they are vapor deposited onto the surface can be approximated by a linear lever rule.[16] The morphology of the interfacial zone in this coverage regime is then heterogeneous with islands of the second reacted phase growing over the first. At the same time, the first phase (or transition

region) grows laterally until the surface is covered at 1 Å. It does not form thereafter, but phase two does.

(3) Coverage range 1—6 Å. In this coverage range, only the TiSi phase forms. As sketched in Fig. 6, islands of TiSi which nucleated at lower coverage coalesce to form a polycrystalline layer. The result is that emission from Si atoms below the TiSi layer is exponentially attenuated.

(4) Coverage range 6—14 Å. This is a region in which the TiSi reaction product is completed and the solid solution of Si in Ti forms. The solution phase grows because the TiSi layer acts as a barrier, preventing the indiffusion of Ti which would continue the disruption of the substrate and release Si. As a result, there are insufficient numbers of Si atoms at the surface to produce the TiSi product. Furthermore, we have observed that Si $2p$ core-level emission changes with coverage in this solution phase, indicating that the concentration of Si decreases with distance from the interface. This concentration profile in any particular Ti crystallite is probably of the form of an error function, as dictated by Fick's laws.

(5) Coverages exceeding ~14 Å. For Ti depositions exceeding a nominal coverage of ~14 Å, a Ti layer forms over the reacted regions with Si content which is below the level of our detectability. This completes the room-temperature evolution of the Ti/Si interface.

These results indicate that a complex, heterogeneous interface is formed at room temperature due to the competition between diffusion and reaction processes at the interface. One must expect that an increase of the substrate temperature would allow more Ti and Si diffusion across the TiSi barrier, and the concentration profile of Fig. 6 would be stretched to higher values of Θ. This diffusion process would reflect the activation energies for grain boundary and bulk diffusion, with the former being the controlling term. Previous work on V/Ge(111) interface formation and thermal properties[13,14] confirmed this expectation in the range $T \leq 300$ °C. For Ti/Si, we have undertaken time-dependent x-ray photoemission studies of diffusion at this interface to investigate the kinetics of this process.[19,30]

Our results suggest that reaction starts as soon as the first Ti atom reaches the semiconductor surface. This is in contrast with the EELS results[21] where an onset of reaction was reported at 2 Å and is more consistent with the MEIS results of Ref. 20 where immediate reaction was observed. In the MEIS study, it was also reported that there was a double layer of "displaced" Si atoms at the interface in a configuration different from the bulk semiconductor. We have found evidence that those displaced atoms can be associated with a reacted or intermixed region rich in Si which is probably $TiSi_4$ in effective composition. Our results also confirm the presence of a TiSi phase up to ~8 Å of Ti, in excellent agreement with the MEIS analysis. At the same time, our ability to resolve chemically inequivalent configurations indicates that a solution phase of variable composition is present in the reacted overlayer.

The Schottky barrier is one of the most important properties of a metal-semiconductor interface for technological application, and it is of importance to relate the Schottky barrier to the chemistry and structure of the interface. In photoemission, studies of the Si $2p$ core level are particularly useful to follow the Schottky-barrier height ϕ_b evolution as a function of metal coverage. Photon energies of 108 and 112 eV provide the bulk sensitivity necessary to distinguish band bending from chemical shifts and the Si $2p$ binding energy can indeed be determined. Here we define $\phi_b = \phi_b(0) + \phi_b(\Theta)$, where $\phi_b(\Theta) = E_c(\Theta) - E_c(0)$, $\phi_b(0)$ is the barrier at the vacuum-silicon interface due to the pinning of the Fermi level by surface states, and E_c is the core-level binding energy. $\phi_b(0)$ can be determined by other measurements to be $\phi_b(0) \cong 0.79$ eV for the Si(111)-2×1 surface.[31,32] In Fig. 7 we show the evolution of ϕ_b for Ti/Si(111) using different symbols to indicate results for different cleaves. As shown, the barrier decreases quickly in the first 1.5—2 Å, achieves a minimum of ~0.54 eV, and increases with increasing coverage to saturate at ~0.68 eV for $10 \leq \Theta \leq 15$ Å.

According to the early Schottky model,[33] the barrier height ϕ_b at a metal-semiconductor junction can be defined as $\phi_b = \phi_M - \chi$, where ϕ_M is the work function of the metal and χ is the difference between the vacuum level and the bottom of the conduction band in the semiconductor. For Si(111), $\chi = 4.2$ eV (Ref. 34) and $\phi_{Ti} = 4.33$ eV.[35] Following the Schottky argument, we should expect then a barrier $\phi_b \sim 0.13$ eV, in contradiction with photoemission, C-V, and I-V measurements.[36] In particular, our results show that a barrier of 0.54 eV is formed when 2 Å of metal are deposited, but that this varies with reaction at the interface.

Many models have been developed to explain discrepancies like this for metal-semiconductor contacts. The importance of defects[37] and interface states has been recognized, but none of these models has been able to quantitatively explain the experimental results. The recent work by Tung *et al.*[38] and Liehr *et al.*[39] with epitaxial $NiSi_2$/Si interfaces has significantly improved our understanding

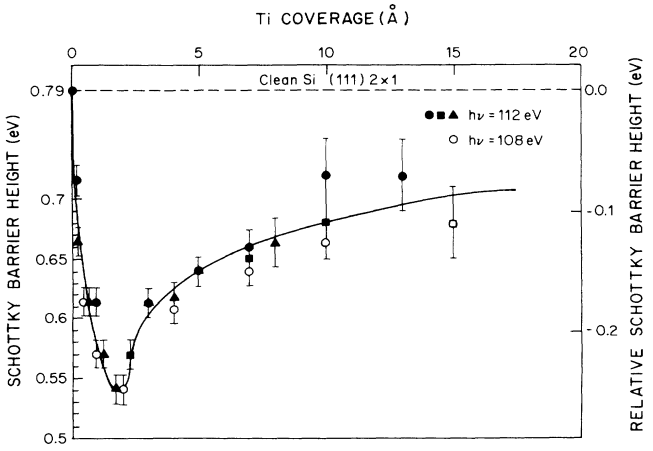

FIG. 7. Relative Schottky-barrier height versus Ti coverage as determined by core-level shifts at $h\nu = 112$ and 108 eV. Different symbols refer to different cleaves. An initial value $\phi_b = 0.79$ eV for the clean n-type Si(111)-2×1 has been assumed (Ref. 32). The changes in the barrier height are correlated to chemical changes at the interface.

of the role of structure and defects. At the same time, we see from Fig. 7 that there are important chemical changes at the interface which alter the barrier height at low coverage.[40]

CONCLUSIONS

We have used high-resolution photoemission results to model the Ti/Si(111)-2×1 interface. The high sensitivity and the relatively large core-level shifts have allowed us to identify and follow the evolution of three reacted species. The first is very close to $TiSi_4$ and constitutes the first few angstroms of the overlayer. The second is a silicide with empirical formula TiSi and is the most extensive part of this interface. The third is a solution of Si in Ti. This graded profile seems to be a common feature for most refractory metal-semiconductor interfaces, where differences are related to the energetics of the reaction products, the character and morphology of the reaction product, and the kinetics of atomic motion through the evolving overlayer. Moreover, we have observed an evolution of the Schottky barrier which parallels changes in the chemistry of the interface.

ACKNOWLEDGMENTS

This work has been supported by the Office of Naval Research under ONR N00014-86-K-0427. The synchrotron-radiation photoemission experiments were done at the University of Wisconsin Synchrotron Radiation Center which is supported by the National Science Foundation. The assistance of the staff of that laboratory is gratefully acknowledged. It is also a pleasure to acknowledge stimulating discussions with R. A. Butera, J. L. Freeouf, K. N. Tu, and O. Aboelfotoh.

[1]G. LeLay, Surf. Sci. **132**, 169 (1983); J. H. Weaver, in *Analysis and Characterization of Thin Films*, edited by K. N. Tu and R. Rosenberg (Academic, New York, in press).
[2]R. Ludeke, Surf. Sci. **132**, 143 (1983).
[3]A. Zunger, Phys. Rev. B **24**, 4372 (1981).
[4]J. H. Weaver, M. Grioni, and J. J. Joyce, Phys. Rev. B **31**, 5348 (1985); J. H. Weaver, A. Franciosi, and V. L. Moruzzi, *ibid.* **29**, 3293 (1984).
[5]P. S. Ho, J. Vac. Sci. Technol. A **1**, 745 (1983).
[6]L. J. Brillson, A. D. Katnani, M. Kelly, and G. Margaritondo, J. Vac. Sci. Technol. A **2**, 551 (1984).
[7]R. Ludeke, J. Vac. Sci. Technol. B **2**, 400 (1984).
[8]A. Franciosi, D. J. Peterman, J. H. Weaver, and V. L. Moruzzi, Phys. Rev. B **25**, 4981 (1982).
[9]R. R. Daniels, A. D. Katnani, G. Margaritondo, and A. Zunger, Phys. Rev. Lett. **47**, 875 (1981).
[10]N. Newman, M. van Shilfgaarde, T. Kendelewicz, M. D. Williams, and W. E. Spicer, Phys. Rev. B **33**, 1146 (1986).
[11]L. J. Brillson, Surf. Sci. Rep. **2**, 123 (1982).
[12]M. del Giudice, J. J. Joyce, M. W. Ruckman, and J. H. Weaver, Phys. Rev. B **32**, 5149 (1985).
[13]M. del Giudice, R. A. Butera, M. W. Ruckman, J. J. Joyce, and J. H. Weaver, J. Vac. Sci. Technol. A **4**, 879 (1986).
[14]M. del Giudice, R. A. Butera, M. W. Ruckman, J. J. Joyce, and J. H. Weaver, in Proc. Mater. Res. Soc., Boston, **54**, 91 (1986).
[15]M. del Giudice, M. Grioni, J. J. Joyce, M. W. Ruckman, S. A. Chambers, and J. H. Weaver, Surf. Sci. **168**, 309 (1986).
[16]R. A. Butera, M. del Giudice, and J. H. Weaver, Phys. Rev. B **33**, 5435 (1986).
[17]M. Grioni, J. J. Joyce, S. A. Chambers, D. G. O'Neill, M. del Giudice, and J. H. Weaver, Phys. Rev. Lett. **53**, 2331 (1984); M. Grioni, J. J. Joyce, M. del Giudice, D. G. O'Neill, and J. H. Weaver, Phys. Rev. B **30**, 7370 (1984).
[18]F. Boscherini, J. J. Joyce, M. W. Ruckman, and J. H. Weaver, Phys. Rev. B **35**, 4216 (1987).
[19]S. A. Chambers, D. M. Hill, F. Xu, and J. H. Weaver, Phys. Rev. B **35**, 634 (1987).
[20]E. J. van Loenen, A. E. M. Fischer, and J. F. van der Veen, Surf. Sci. **155**, 65 (1985).
[21]M. Iwami, S. Hashimoto, and A. Hiraki, Solid State Commun. **49**, 459 (1984).
[22]R. Butz, G. W. Rubloff, T. Y. Tan, and P. S. Ho, Phys. Rev. B **30**, 5421 (1984).
[23]R. M. Walser and R. W. Bené, Appl. Phys. Lett. **28**, 624 (1976); M. Ronay, *ibid.* **42**, 577 (1983).
[24]M. O. Aboelfotoh and K. N. Tu, Phys. Rev. B **33**, 6572 (1986); **34**, 2311 (1986).
[25]G. Margaritondo, N. G. Stoffel, and J. H. Weaver, J. Phys. E **12**, 602 (1979).
[26]S. Brennan, J. Stöhr, R. Jaeger, and J. E. Rowe, Phys. Rev. Lett. **45**, 1414 (1980).
[27]F. J. Himpsel, P. Heimann, T.-C. Chiang, and D. E. Eastman, Phys. Rev. Lett. **45**, 1112 (1980); F. J. Himpsel, D. E. Eastman, P. Heimann, B. Reihl, C. W. White, and D. M. Zehner, Phys. Rev. B **24**, 1120 (1981).
[28]K. C. Pandey, Phys. Rev. Lett. **47**, 1913 (1981); D. R. Hamann, Surf. Sci. **68**, 167 (1977); D. E. Eastman, J. Vac. Sci. Technol. **17**, 492 (1980).
[29]M. P. Seah and W. A. Dench, Surf. Interface Anal. **1**, 2 (1979).
[30]R. M. Tromp, G. W. Rubloff, and E. J. van Loenen, J. Vac. Sci. Technol. A **4**, 865 (1986).
[31]F. G. Allen and G. W. Gobels, Phys. Rev. **127**, 150 (1962); C. Sebenne, D. Bolmont, G. Guichar, and M. Balkanski, Phys. Rev. B **12**, 3280 (1975).
[32]J. G. Clabes, G. W. Rubloff, B. Reihl, R. J. Purtell, P. S. Ho, A. Zartner, F. J. Himpsel, and D. E. Eastman, J. Vac. Sci. Technol. **20**, 684 (1982).
[33]W. Schottky, Z. Phys. **118**, 539 (1942).
[34]C. A. Sébenne, Nuovo Cimento **39B**, 768 (1977).
[35]M. Weinert and R. E. Watson, Phys. Rev. B **29**, 3001 (1984); H. B. Michaelson, J. Appl. Phys. **48**, 4729 (1977).
[36]J. L. Freeouf, Surf. Sci. **132**, 233 (1983).
[37]W. E. Spicer, P. W. Chye, P. R. Skeath, C. Y. Su, and I. Lindau, J. Vac. Sci. Technol. **16**, 1422 (1979).
[38]R. Tung, J. M. Gibson, and J. M. Poate, Phys. Rev. Lett. **50**, 429 (1983).
[39]M. Liehr, P. E. Schmid, F. K. LeGoues, and P. S. Ho, Phys. Rev. Lett. **52**, 461 (1985).
[40]J. L. Freeouf and J. M. Woodall, Appl. Phys. Lett. **39**, 727 (1981).